

CFD Based on The Visualisation of Aortic Valve Mechanism in Aortic Valve Stenosis for Risk Prediction at The Peak Velocity

Nur' Afifah Yousri¹, Nabilah Ibrahim^{1,*}, Nur Amani Hanis Roseman², Ishkrizat Taib², Shahnoor Shanta³

- ¹ Department of Electrical and Electronic Engineering, Faculty of Electrical and Electronic Engineering, Universiti Tun Hussein Onn Malaysia, 86400 Batu Pahat, Johor, Malaysia
² Department of Mechanical & Manufacturing Engineering, Faculty of University Tun Hussein Onn Malaysia, 86400 Batu Pahat, Johor, Malaysia
³ Computer and Information Sciences, Harrisburg University of Science and Technology, PA 17101, USA

ARTICLE INFO

Article history:

Received 5 December 2023
Received in revised form 1 January 2024
Accepted 18 February 2024
Available online 30 March 2024

Keywords:

Aortic valve stenosis; computational fluid dynamics (CFD); Navier-Stokes equation; hemodynamic parameters

ABSTRACT

Aortic valve disease plays a crucial role in the development of cardiovascular disease (CVD), leading to increased rates of mortality and morbidity. Two diseases, aortic valve regurgitation and aortic valve stenosis are known to occur in the aortic valve. However, aortic valve stenosis is gaining attention due to its severe impact on the patient. The malfunction of the aortic valve might be affected by blood flow, which leads to stenosis. This study aims to investigate the blood flow re-circulation on the aortic valve in different stenotic regions when the blood's velocity reaches the peak flow of the time in the systole phases. Four different models of aortic valve stenotic are designed using computer-aided design (CAD) software. The computational fluid dynamics (CFD) approach governed by the Navier-Stokes equation is imposed to identify the characteristics of the blood backflow at the left ventricle. Several hemodynamic factors are considered, such as time-averaged wall shear stress (TAWSS), oscillatory shear index (OSI) and relative residence time (RRT). The blood flow characteristic is expected to be chaotic, especially at the highest percentages of aortic valve stenosis, presenting the worst condition to the heart. This finding supports healthcare providers in foreseeing the deterioration of the patient's condition and opting for aorta valve surgery replacement.

1. Introduction

Nowadays, the global population is exposed to the danger of cardiovascular disease (CVD), regardless of age. The population at risk for CVD includes individuals who are ageing, as this disease is a leading cause of death globally [1]. According to the World Health Organization (2019), coronary artery disease is a type of cardiovascular disease (CVD) that contributes to 32% of global deaths, with heart attack and stroke accounting for 85% of these fatalities [2]. Furthermore, in 2018, Malaysia reported coronary artery disease as the top cause of mortality within the 100,000 population and is ranked 64th worldwide [3]. Aortic valve stenosis is one of the most common and serious aortic valve

* Corresponding author.

E-mail address: nabilah@uthm.edu.my

<https://doi.org/10.37934/armne.17.1.5668>

diseases in CVD because of progressive fibrocalcification and thickening of aortic valve cusps that lead to the narrowing of valve opening [4]. It is reported in other studies that aortic valve disease cases are most likely to develop high blood pressure and lead to heart failure [5]. Echocardiogram, cardiac magnetic resonance imaging (MRI), and cardiac CT scan are the diagnostic tools used in hospitals to detect aortic valve complications [6]. Patients who are financially burdened may view these methods as costly, causing them to lose motivation in addressing their aortic valve stenosis and increasing the risk of a fatal outcome [5].

Brown *et al.*, stated that two prevailing treatment options used to determine the long-term survival and reoperation necessity in patients with an asymptomatic aortic valve are surgical aortic valve replacement (SAVR) and transcatheter aortic valve replacement (TAVR) [7]. Instead of SAVR and TAVR, medical officers typically rely on computational analysis methods to assess the condition of asymptotic aortic valves through echocardiogram images. This study collected the geometry of the normal and asymptotic aortic root that consists of sinotubular junction (STJ), leaflet thickness, valve height, leaflet length and aortoventricular junction (AVJ) from the previous study. Five asymptotic aortic valve models have been designed using computer-aided design (CAD) based on valve thickness and valve orifice differences. Besides modelling on the CAD software, the analysis was carried out using computational fluid dynamics (CFD) simulation. Mokhtar and Aizat utilised CFD software to simulate a blood flow pattern, velocity and vorticity using the continuity equation and Navier-Stokes equations [8]. Based on the findings from the previous paper, Zhu *et al.*, found that the data are accurate and convenient to practise in simulation [9]. Meanwhile, Basri *et al.*, employed the combination of MRI and CFD as a powerful method for discerning the valve opening and its influence on hemodynamics in the blood flow of the aortic valve [10]. Thus, this study will use the CFD simulation to analyse the velocity and pressure of the blood flow in the peak flow of systole phases. Three hemodynamic factors were implemented in this study, which consists of time average wall shear stress (TAWSS), oscillatory shear index (OSI), and relative residence time (RRT).

2. Methodology

This study proposes the mechanism and behaviour of aortic valve stenosis through numerical simulation. This method assesses aortic valve mechanism and behaviour in two conditions: normal aortic valve and asymptotic aortic valve. Firstly, the valve's geometry is designed via SOLIDWORKS. Here, several geometries of the aortic valve in different stenotic areas are developed by setting up the variables collected from the literature. Subsequently, an investigation is carried out to analyse and observe the blood flow pattern simulation on different stenotic regions of the aortic valve, aiming to explore the potential stages that may occur in aortic valve stenosis disease. The blood flow characteristics are then analysed by providing statistical calculations on flow re-circulation or backflow signs for the stenotic aortic valve.

2.1 Development of The Simulation Aortic Valve in CFD Simulation

Figure 1 shows a block diagram illustrating the aortic valve simulation in CFD. Initially, simplifying a geometry model is necessary before initiating the meshing process. Figure 2 shows the boundary condition of the inlet, wall and outlet (Canonsburg, Pennsylvania, United States). The element size of the mesh is set up based on the parameter that was decided earlier. Figure 3 shows the tetrahedrons method that was applied due to the accuracy of mesh quality during the evaluation of the elements and nodes on the meshing model. The nodes from the tetrahedral meshing reported a mesh size of

99782, with 550640 elements. The skewness of the model is 0.8. The blood density and viscosity values are 1060 kg/m^3 and 0.0035 Pa.s , respectively.

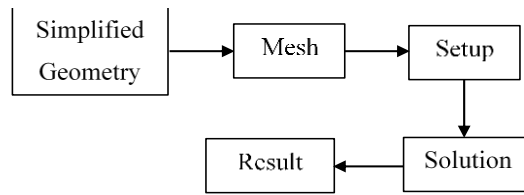


Fig. 1. Block diagram in fluid flow

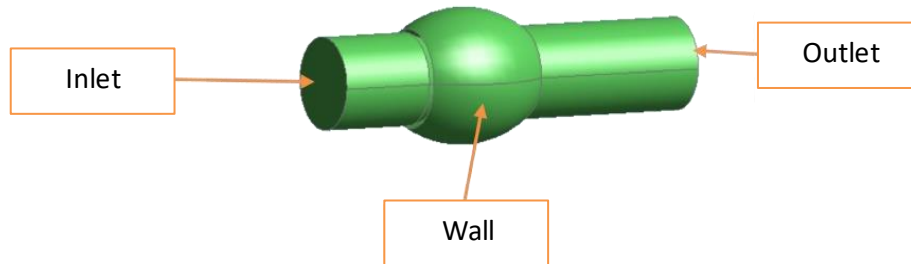


Fig. 2. Boundary condition

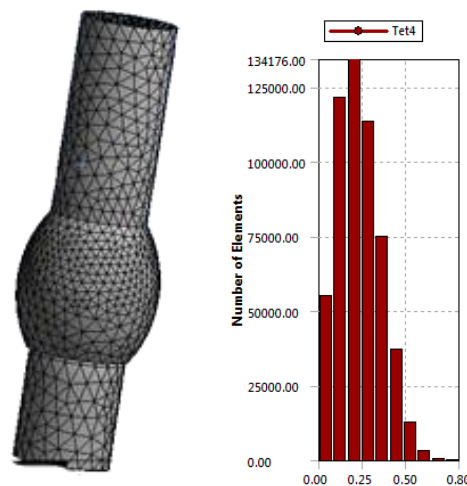


Fig. 3. Meshing process

2.2 The Geometry of Normal and Asymptotic Aortic Valve

2.2.1 Schematic diagram of the aortic root

Figure 4 shows the schematic diagram of the aortic valve. Three variable parameters are to be considered to visualise the blood flow in normal and asymptotic aortic valves: valve orifice, valve cusps thickness, and inlet velocity, as shown in Figure 4. In addition, those parameters were calculated by 100%, 70%, 50%, and 30% based on a normal aortic valve.

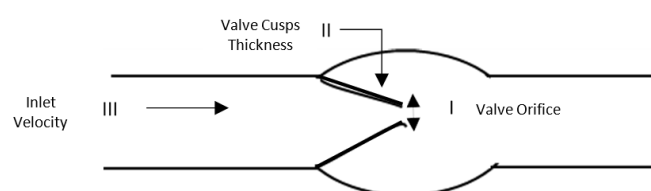
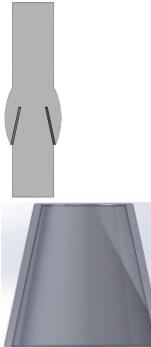
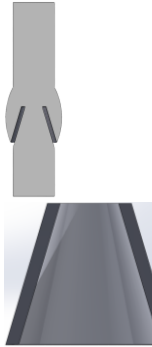
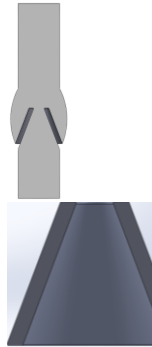


Fig. 4. Schematic diagram of aortic valve

2.2.2 Geometry of the 2D simplified model in the condition of normal and asymptotic aortic valve

Table 1 shows the simplified geometry of the valve orifice and the valve thickness of the aortic valve, where the smaller valve orifice would produce a larger plaque built at the valve leaflet. In this study, the parameters of the aortoventricular junction, sinus of valsava, the height of the valve, and leaflet length are fixed at 17mm, 22mm, 17mm, and 17mm, respectively. Meanwhile, the valve orifice's opening is varied at 100%, 70%, 50% and 30% while its corresponding thickness is set at 14mm and 0.5mm, 9.8mm and 0.9mm, 7mm and 1.5mm, and 4.2 mm and 1.8 mm, respectively.

Table 1
 Difference percentage of valve orifice and valve thickness of normal and asymptotic aortic valve

	Normal aortic valve	Asymptotic aortic valve (Stenosis)		
The percentage of the aortic valve when opening (Systole Phases) Model design focusing on aortic valve location	100%	70%	50%	30%
Various valve orifice and the valve thickness				

2.2.3 Grid independence test (GIT) on the simplified model in the condition of normal and asymptotic aortic valve

Grid independence test (GIT) was conducted to identify the influence of grid size on the accuracy and reliability of their simulation result on aortic valve stenosis could be accessed [11]. GIT was performed in these four simplified models where only tetrahedron meshes were considered due to their ability to conform to complex geometries, such as aortic valves, which are more effective than other meshes [10]. Based on Table 2, there are 9 GIT that have been done during the simulation. It involved total nodes, total elements, and element sizes. The element size of this study is 0.8 mm. Figure 5 shows a graph of nine GIT calculated before conducting the simulation in Ansys. The graph shows that the velocity differences between git6, git7, git8, and git9 diminish to zero, signifying higher reliability when utilising these amount of elements in the four simplified models.

Table 2
 List of nodes, elements and the size of element of 9 GIT

	Nodes	Elements	Size of element
GIT1	101715	560322	3.5
GIT2	102861	565607	2.0
GIT3	117337	638876	1.0
GIT4	123033	668161	0.9
GIT5	126896	688385	0.85
GIT6	129231	700687	0.82
GIT7	131422	712180	0.8
GIT8	133498	723109	0.78
GIT9	137113	742155	0.75

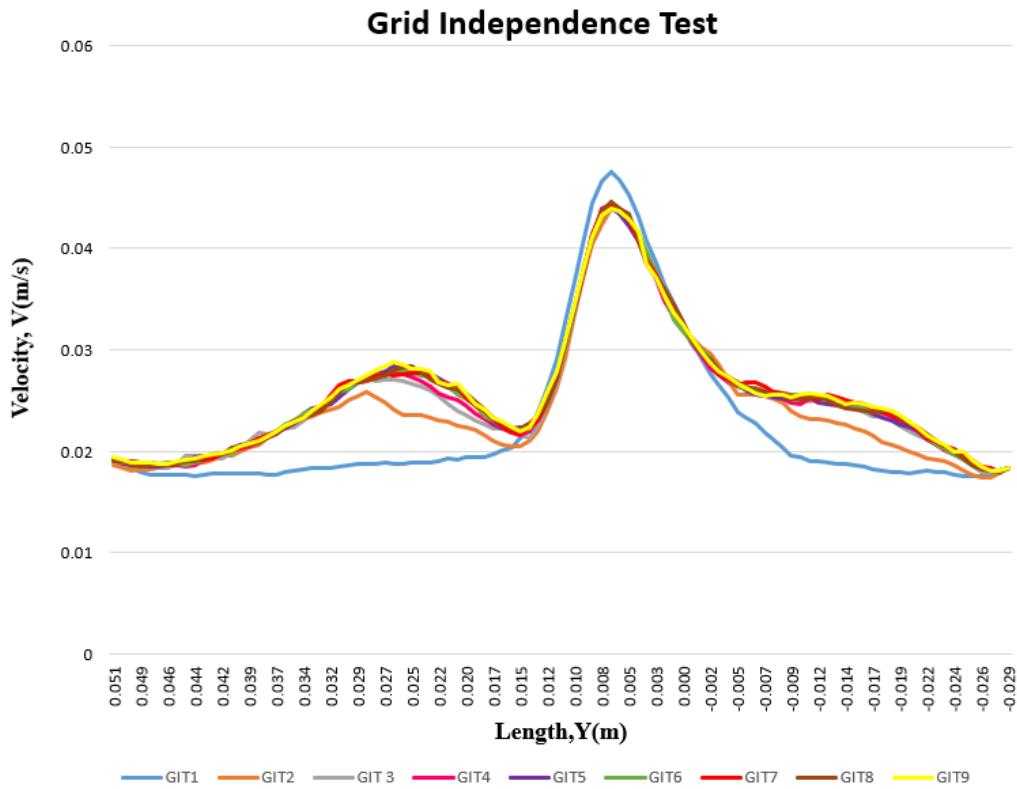


Fig. 5. The graph of the grid independence of the relationship between velocity (m/s) and the length of aortic root (m) that have been stimulated and calculated to get the stable data for determining the mesh value

2.3 Governing Equation

Computational fluid dynamics (CFD) simulation involves the Navier-Stokes equations, which include the conservation of momentum (see Eq. (1)), and the Continuity equation, which ensures the mass conservation principle (see Eq. (2)). These two equations are fundamental for modelling a blood flow through aortic valve [13,14]. Assuming the blood behaves as a Newtonian and incompressible fluid, the Navier-Stokes equation can be described as

$$\rho \frac{\delta u}{\delta t} + \rho(u \cdot \nabla)u = -\nabla p + \mu \nabla^2 u \quad (1)$$

$$\nabla \cdot u = 0 \quad (2)$$

where u represents velocity, p is pressure, ρ denotes density, and μ stands for viscosity. Each variable plays a crucial role in capturing blood flow dynamics through the aortic valve [13].

2.4 Boundary Condition and Parameter Assumption

In this study, the identification of blood flow as laminar or turbulent was achieved by checking its Reynold number, as defined in Eq. (3). Moreover, the flow is classified as laminar when the Reynold number $Re \leq 2000$ and it is deemed turbulent when the Reynold number $Re \geq 3000$ [13].

$$Re = \frac{\rho V D}{\mu} \quad (3)$$

ρ represents the blood density, V stands for velocity, D denotes the diameter of the aortic root, and μ represents viscosity. In this context, the blood density and viscosity are constants, remaining unchanged throughout the calculations. At the peak velocity (0.12s), the Reynold number is 5148.5714, greater than 3000, generating a turbulent flow. Furthermore, the simulated blood was considered an incompressible Newtonian fluid [12] with constant viscosity and blood density values of 0.0035 Pa and 1060kg/m³, respectively. The aortic root wall was considered rigid, and a non-slip boundary condition was applied along its surface.

Three boundary conditions have been set up in the aortic valve model: inlet, wall and outlet. The selection of inlet and outlet is important to avoid the backflow of blood in the region of the aortic valve. Figure 6 shows a diagram of boundary conditions in the aortic valve being set up before the analysis in CFD simulation. Meanwhile, Table 3 describes the boundary conditions used in these simplified models.

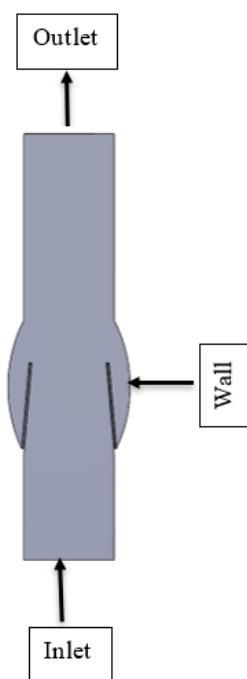


Fig. 6. Diagram of boundary condition in Aortic valve

Table 3
 Boundary conditions in the modelling

	Inlet	Outlet	Walls
Boundary condition	Physiological velocity inlet in aortic valve	Physiological pressure outlet from the velocity inlet	Solid walls for aortic root and sinuses of Valsalva (surrounded at aortic valve)

2.5 The Hemodynamic Parameters of Aortic Valve Model

There are two phases involved in a cardiac cycle: systolic and diastolic [14]. This study focuses on the systole phases in the peak-flow time of inlet velocity, where the aortic valve condition is fully open to ensure the oxygenated blood passes through from the left ventricle to the whole body. This study used Ansys software to measure the velocity, pressure, and hemodynamic parameters of normal and asymptotic aortic valves with stenosis. The hemodynamic parameters involved are Wall

Shear Stress (WSS), Oscillatory Shear Index (OSI) and Relative Residence Time (RRT) that focus the blood flow on the vessel wall, oscillating shear forces and duration of the blood spent to pass through the valve, respectively. Thus, CFD software assesses all the parameters to observe the visualisation of the blood flow between normal and asymptotic aortic valves.

3. Result and Discussion

3.1 Visualisation of The Blood Flow Characteristic Effect Geometry of Normal and Asymptotic Aortic Valve in Terms of Velocity and Pressure

The velocity and pressure in the aortic valve are important parameters in assessing the functional state of the valve and determining the severity of aortic valve disease. It also shows the blood flow and pressure in the blood vessel due to different percentages of the stage level thickness of the valve and valve orifice. Besides that, there are several hemodynamic parameters, including Time-averaged Wall Sheer Stress (TAWSS), Oscillatory Sheer Index (OSI) and Relative Residence Time (RRT), which were used to determine the flow of blood through the wall and predict the risk condition of the Aortic Root. Here, the Velocity, Pressure, Time-averaged Wall Sheer Stress (TAWSS), Oscillatory Sheer Index (OSI) and Relative Residence Time (RRT) of the blood flow are presented.

a) Velocity

All normal and stenotic conditions of the aortic valve have been set up in the same inlet velocity. This study focused on the peak velocity during the systole phase. The peak hours that occur in the aortic root is in 0.12s. Table 4 shows the velocity contour in the designated aortic valve at different stenotic valve openings of 100%, 70%, 50% and 30%. The normal aortic valve's flow is more stable than the other three conditions due to the absence of plaque at the valve. Meanwhile, for 70%, 50% and 30% of the stenotic valve, the velocity shows instability and fluctuates after the blood flow from the aortic valve. The instability is contributed by the formation of plaque at the valve cusps and the orifice of the valve. In addition, 30% of stenotic aortic valves manifest the highest blood flow velocity through the aortic valve compared to 50% and 70% of stenotic aortic valves. The velocity hike is due to its smallest diameter of valve orifice and thickness at 4.2mm and 1.8mm, respectively.

Figure 7(a) shows the relationship between the AB line distance, and Figure 7(b) shows the velocity graph of the blood flow through the aortic root. The graph shows the effect of the aortic valve opening percentage on the flow velocity at 0.12s of peak systole. The resulting graph was obtained along the line AB (from the inlet to the outlet). The 100% opening valve model shows a stable graph, which means that the blood flow through the aortic valve did not have any obstacles, such as a plaque or the smallest orifice. Meanwhile, the velocity fluctuates for 70%, 50%, and 30% of the stenotic valves in the wake of the stenotic valve. As a result, the velocity fluctuation was higher in 30% compared to 70% and 50% due to plaque build-up, resulting in a smaller valve orifice and increased blood velocity after the aortic valve.

Table 4

The velocity of the blood flow through the aortic root in different sizes of the valve orifice and the thickness of the valve

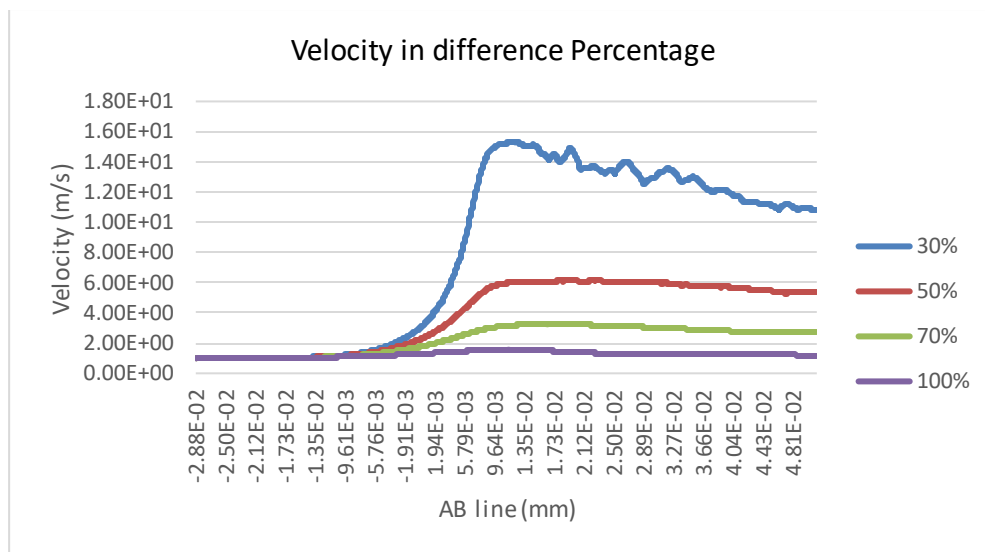
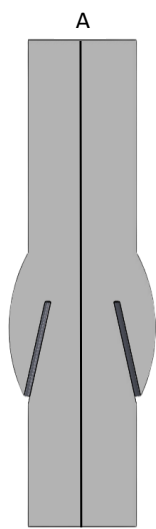
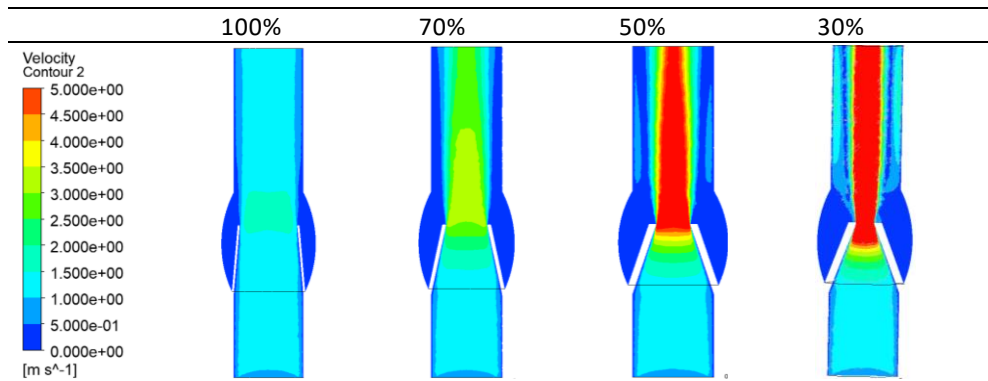
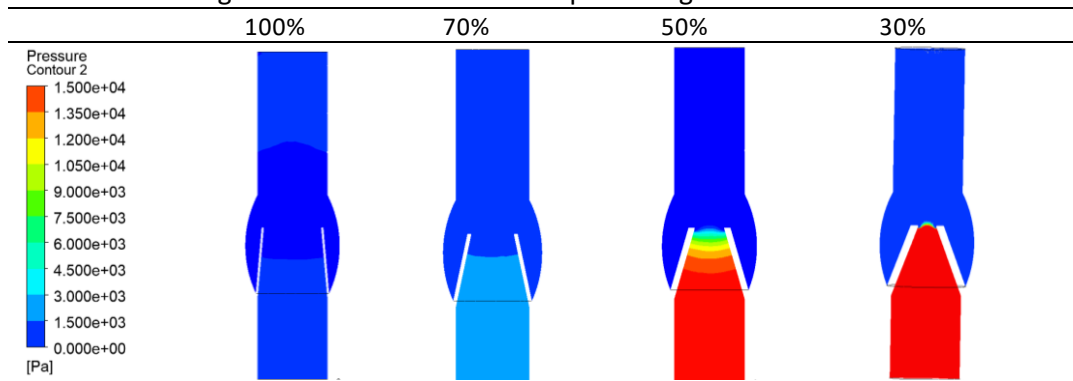


Fig. 7. (a) AB line is a line along the centre of the aortic root (b) The velocity that occurs in the peak value of inlet velocity when the time is in 0.12s that occur in four difference percentage of stenotic aortic valve

b) Pressure

The pressure contours for the simplified aortic valve model are shown in Table 5, comparing the normal condition to the condition with stenosis. Calcification of the plaque results in a higher pressure as expected, and the pressure between the inlet and outlet of the aortic valve is different [15]. The contour result showed that a smaller valve orifice would produce higher pressure at the aortic valve. The elevation in pressure is caused by the heart working harder when the opening narrows and the plaque thickens. Due to the absence of plaque on the aortic valve wall, the pressure remains low for the normal valve with a wide opening. Meanwhile, as the valve orifice becomes smaller, there is a gradual increase in pressure at the blood inlet due to the plaque becoming increasingly high at 70%, 50%, and 30%.

Table 5
 Pressure flowing in aortic root on difference percentage valve stenotic



3.2 Hemodynamic Effect on Different Percentages of Aortic Valve During Systolic Phase a) Time average wall shear stress (TAWSS)

Wall shear stress and time-averaged wall shear stress (TAWSS) are essential parameters to consider in the context of aortic valve stenosis [16]. It refers to the tangential force per unit surface area exerted by flowing blood on the vessel wall [17]. Endothelial cells positioned at the interface of the blood vessel wall are responsible for detecting this force, which has the potential to be utilised as a biomarker for cardiovascular disorders like atherosclerosis, aneurysm, and aortic valve stenosis [18]. A malfunctioning aortic valve causes altered blood flow patterns and higher wall shear stress in the proximal aorta in aortic valve stenosis patients [18]. TAWSS, on the other hand, represents the average wall shear stress magnitude over an entire cardiac cycle. The calculation and analysis of TAWSS in the aortic valve can provide valuable insight into hemodynamic changes occurring in the disease's aorta and their potential impact on vascular function and wall progression [15]. The time-averaged wall shear stress (TAWSS) can be estimated as shown in Eq. (4). TAWSS can be calculated by integrating the instantaneous wall shear stress values over one cardiac cycle [19].

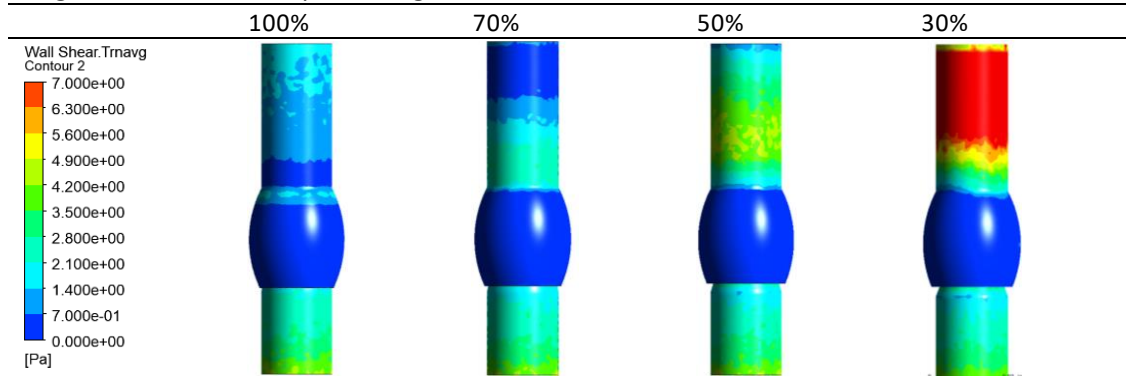
$$TAWSS = \frac{1}{T} \int_0^T |WSS_i| dt \quad (4)$$

where WSS is wall shear stress, WSS_i is the instantaneous wall shear stress, and T donates the duration of one cardiac cycle [19].

By analysing TAWSS, the impact of the blood flow at the wall at the aortic root, as shown in Table 6, could be visualised. The outcome demonstrates the effect of blood flow through the aortic valve on the wall, ranging from a healthy to the most severe model of the aortic root. Here, the blue contour defines the lowest value of TAWSS, and the red one represents the highest value. When the blood flow velocity increases during the decrease of the valve orifice size, TAWSS produces high stress, indicating that the vessel wall region is experiencing sustained elevated shear force. This TAWSS spike led to the risk of aortic valve stenosis progression and complications.

Table 6

Contour of the impact at the wall shear stress in time average (TAWSS) after the aortic valve segment in difference percentage of stenotic



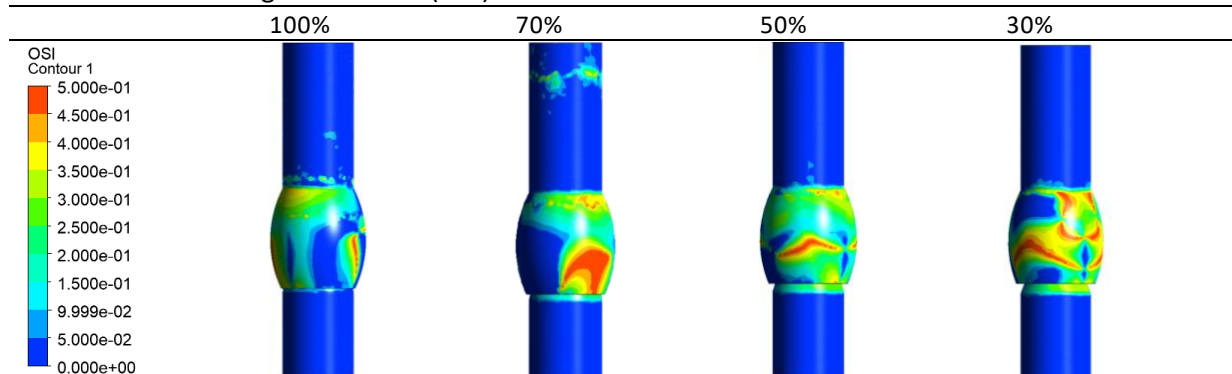
b) Oscillatory shear index (OSI)

The oscillating shear index (OSI) at the wall is calculated based on the wall shear stress vector and represents the magnitude of the oscillating shear forces experienced by the aortic valve [20]. These forces can play a role in the progression of aortic valve disease, affecting the valve’s structural integrity and overall function [21]. Thus, OSI of the aortic valve is one of the crucial indexes for assessing its health and function. High OSI values imply increased oscillatory shear forces, which can contribute to endothelial dysfunction. Meanwhile, unidirectional flow was assigned with a low OSI value [22]. Table 7 shows the OSI occurring at the wall in the different conditions of the aortic valve. High OSI is observed in the wall when the percentage of aortic valve opening is low, as indicated by the OSI contour. Therefore, monitoring and evaluating the OSI of aortic can provide valuable insights into its hemodynamics and potential risk for developing cardiovascular complications. The equation applied in estimating the OSI is presented as follows

$$OSI = \frac{1}{2} \left(1 - \frac{\left| \int_0^T WSS dt \right|}{TAWSS} \right) \tag{5}$$

Table 7

Contour of oscillating shear index (OSI) at the wall of aortic root that occur at the wall of aortic valve



c) Relative residence time (RRT)

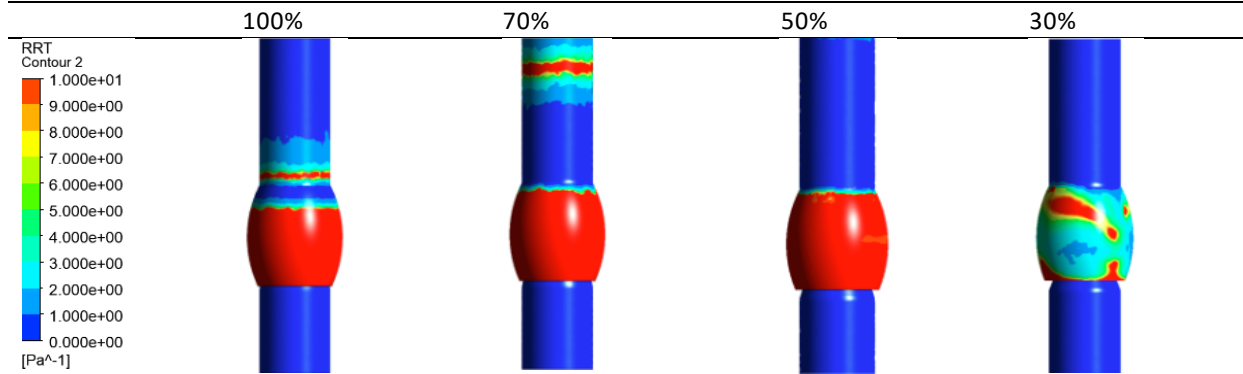
The relative residence time (RRT) at the aortic root of the aortic valve is another essential factor in understanding the progression and consequences of various conditions affecting the valve [23]. It

is influenced by factors such as the degree of the valve narrowing, the resistance to blood flow and hemodynamic changes caused by increased wall shear stress (WSS) [24]. RRT also refers to the duration of the blood spent to pass through the valve during each cardiac cycle. When the aortic valve becomes stenosed, the RRT increases, leading to prolonged exposure to the worst condition, while low RRT is associated with a healthier functioning valve. The equation used in RRT is shown in Eq. (6). Based on the calculation, the RRT becomes low when TAWSS and OSI are at higher values, as shown in Table 8. In addition, the diameter of the valve orifice is proportional to the RRT. This is due to the high pressure affected before the valve orifice that makes the resident time of blood leaving the area low. As a result, the blood's backflow and plaque formation at the valve occur. In this case, the 30% stenotic valve model shows the lowest RRT that forms more plaque around the valve.

$$RRT \sim \frac{1}{TAWSS(1-2OSI)} \tag{6}$$

Table 8

Contour of relative residence time (RRT) at the wall of aortic root that occur at the wall of aortic valve



4. Conclusion

The purpose of this study is to visualise the normal and stenotic aortic valve condition using the CFD program. Four conditions in this study involve the aortic valve opening of 100%, 70%, 50%, and 30%. The geometry of this study is obtained from the previous work on the normal condition of the aortic valve, and the percentage of the worst conditions (containing stenosis) is calculated from the healthy condition. The results discussed the velocity, pressure, and hemodynamic parameters of the blood flow characteristic effect geometry of aortic valve in different valve thicknesses and valve orifice. The contour scale of the velocity across the four models of the aortic valve shows an increment in colour and fluctuation in the velocity graph as the valve orifice became smaller and the plaque became thicker. In addition, the opening of the valve orifice plays a crucial role in causing fluctuations in blood flow, particularly in patients with aortic valve stenosis. Regarding the pressure parameter in the stenotic aortic valve model, pressure rises as blood force occurs in the inlet aortic root, but subsequently drops after the blood passes through the region of the aortic valve, leading to increased velocity. Moreover, the observation of TAWSS, OSI and RRT could assist the physician in predicting early diagnosis of the heart condition.

To conclude, the study provided valuable insights into the complex nature of blood flow in the aortic valve and visualisation of the blood flow patterns on the aortic valve. This visual data of the contour serves as a valuable resource for further analysis and can aid in the diagnosis and prediction treatment of the aortic valve.

Acknowledgment

This research was supported by Universiti Tun Hussein Onn Malaysia (UTHM) through TIER 1 (vot Q542) and for GPPS Vot Q220.

Reference

- [1] Sazlina, Shariff Ghazali, Rajini Sooryanarayana, Bee Kiau Ho, Mohd Azahadi Omar, Ambigga Devi Krishnapillai, Noorlaili Mohd Tohit, Sheleaswani Inche Zainal Abidin, Suthahar Ariaratnam, and Noor Ani Ahmad. "Cardiovascular disease risk factors among older people: Data from the National Health and Morbidity Survey 2015." *PLoS One* 15, no. 10 (2020): e0240826. <https://doi.org/10.1371/journal.pone.0240826>
- [2] World Health Organization. "Cardiovascular disease." http://www.who.int/cardiovascular_diseases/en/ (2017).
- [3] Health profile Malaysia. "World Life Expectancy." <https://www.worldlifeexpectancy.com/country-health-profile/malaysia>
- [4] Setiawan, Noor Akhmad, Paruvachi Ammasai Venkatachalam, and Ahmad Fadzil M. Hani. "Diagnosis of coronary artery disease using artificial intelligence based decision support system." *arXiv preprint arXiv:2007.02854* (2020).
- [5] Nowak, Marcin, Eduardo Divo, and Wojciech P. Adamczyk. "Fluid–Structure Interaction methods for the progressive anatomical and artificial aortic valve stenosis." *International Journal of Mechanical Sciences* 227 (2022): 107410. <https://doi.org/10.1016/j.ijmecsci.2022.107410>
- [6] Apostolakis, Efstratios, Nikolaos A. Papakonstantinou, Nikolaos G. Baikoussis, Anastasios Petrou, and John Goudevenos. "Imaging of acute aortic syndrome: advantages, disadvantages and pitfalls." *Hellenic J Cardiol* 56, no. 2 (2015): 169-80.
- [7] Brown, Bailey, Tan Le, Aroma Naeem, Aroosa Malik, Elizabeth L. Norton, Xiaoting Wu, Himanshu J. Patel, G. Michael Deeb, Karen M. Kim, and Bo Yang. "Stentless valves for bicuspid and tricuspid aortic valve disease." *JTCVS open* 8 (2021): 177-188. <https://doi.org/10.1016/j.xjon.2021.09.033>
- [8] Mokhtar, N. Hafizah, and Aizat Abas. "Simulation of Blood flow in Artificial Heart Valve Design through Left heart." In *IOP Conference Series: Materials Science and Engineering*, vol. 370, no. 1, p. 012066. IOP Publishing, 2018. <https://doi.org/10.1088/1757-899X/370/1/012066>
- [9] Zhu, Yulei, Rui Chen, Yu-Hsiang Juan, He Li, Jingjing Wang, Zhuliang Yu, and Hui Liu. "Clinical validation and assessment of aortic hemodynamics using computational fluid dynamics simulations from computed tomography angiography." *Biomedical engineering online* 17 (2018): 1-12. <https://doi.org/10.1186/s12938-018-0485-5>
- [10] Basri, Adi A., Mohamed Zubair, Ahmad FA Aziz, Rosli M. Ali, Masaaki Tamagawa, and Kamarul A. Ahmad. "Computational fluid dynamics study of the aortic valve opening on hemodynamics characteristics." In *2014 IEEE Conference on Biomedical Engineering and Sciences (IECBES)*, pp. 99-102. IEEE, 2014. <https://doi.org/10.1109/IECBES.2014.7047660>
- [11] Zbavitel, Jan, and Simona Fialová. "A numerical study of hemodynamic effects on the bileaflet mechanical heart valve." In *EPJ Web of Conferences*, vol. 213, p. 02103. EDP Sciences, 2019. <https://doi.org/10.1051/epjconf/201921302103>
- [12] Caballero, Andres D., and S. J. C. E. Laín. "A review on computational fluid dynamics modelling in human thoracic aorta." *Cardiovascular Engineering and Technology* 4 (2013): 103-130. <https://doi.org/10.1007/s13239-013-0146-6>
- [13] Zhu, Yulei, Rui Chen, Yu-Hsiang Juan, He Li, Jingjing Wang, Zhuliang Yu, and Hui Liu. "Clinical validation and assessment of aortic hemodynamics using computational fluid dynamics simulations from computed tomography angiography." *Biomedical engineering online* 17 (2018): 1-12. <https://doi.org/10.1186/s12938-018-0485-5>
- [14] Leo, Hwa-Liang, Hélène Simon, Josie Carberry, Shao-Chien Lee, and Ajit P. Yoganathan. "A comparison of flow field structures of two tri-leaflet polymeric heart valves." *Annals of Biomedical Engineering* 33 (2005): 429-443. <https://doi.org/10.1007/s10439-005-2498-z>
- [15] Salman, Huseyin Enes, Levent Saltik, and Huseyin C. Yalcin. "Computational analysis of wall shear stress patterns on calcified and bicuspid aortic valves: Focus on radial and coaptation patterns." *Fluids* 6, no. 8 (2021): 287. <https://doi.org/10.3390/fluids6080287>
- [16] Yevtushenko, Pavlo, Leonid Goubergrits, Benedikt Franke, Titus Kuehne, and Marie Schafstedde. "Modelling blood flow in patients with heart valve disease using deep learning: A computationally efficient method to expand diagnostic capabilities in clinical routine." *Frontiers in Cardiovascular Medicine* 10 (2023): 1136935. <https://doi.org/10.3389/fcvm.2023.1136935>
- [17] Shokina, Nina, Gabriel Teschner, Andreas Bauer, Cameron Tropea, Herbert Egger, Jürgen Hennig, and Axel J. Krafft. "Parametric Sequential Method for MRI-Based Wall Shear Stress Quantification." *IEEE Transactions on Medical Imaging* 40, no. 4 (2020): 1105-1112. <https://doi.org/10.1109/TMI.2020.3046331>

- [18] Gross, Tatiana M. Sequeira, Diana Lindner, Francisco M. Ojeda, Johannes Neumann, Nimrat Grewal, Thomas Kuntze, Stefan Blankenberg, Hermann Reichenspurner, Dirk Westermann, and Evaldas Girdauskas. "Comparison of microstructural alterations in the proximal aorta between aortic stenosis and regurgitation." *The Journal of thoracic and cardiovascular surgery* 162, no. 6 (2021): 1684-1695. <https://doi.org/10.1016/j.jtcvs.2020.03.002>
- [19] Lee, Ui Yun, Gyung Ho Chung, Jinmu Jung, and Hyo Sung Kwak. "Size-dependent distribution of patient-specific hemodynamic factors in unruptured cerebral aneurysms using computational fluid dynamics." *Diagnostics* 10, no. 2 (2020): 64. <https://doi.org/10.3390/diagnostics10020064>
- [20] Geeraert, Patrick, Fatemehsadat Jamalidinan, Ali Fatehi Hassanabad, Alireza Sojoudi, Michael Bristow, Carmen Lydell, Paul WM Fedak, James A. White, and Julio Garcia. "Bicuspid aortic valve disease is associated with abnormal wall shear stress, viscous energy loss, and pressure drop within the ascending thoracic aorta: A cross-sectional study." *Medicine* 100, no. 26 (2021). <https://doi.org/10.1097/MD.00000000000026518>
- [21] Shimoni, Sara, Iris Bar, Valery Meledin, Estela Derazne, Gera Gandelman, and Jacob George. "Circulating endothelial progenitor cells and clinical outcome in patients with aortic stenosis." *PLoS One* 11, no. 2 (2016): e0148766. <https://doi.org/10.1371/journal.pone.0148766>
- [22] Goody, Philip Roger, Mohammed Rabiul Hosen, Dominik Christmann, Sven Thomas Niepmann, Andreas Zietzer, Matti Adam, Florian Bönner, Sebastian Zimmer, Georg Nickenig, and Felix Jansen. "Aortic valve stenosis: from basic mechanisms to novel therapeutic targets." *Arteriosclerosis, thrombosis, and vascular biology* 40, no. 4 (2020): 885-900. <https://doi.org/10.1161/ATVBAHA.119.313067>
- [23] Plunde, Oscar, and Magnus Bäck. "Fatty acids and aortic valve stenosis." *Kardiologia Polska (Polish Heart Journal)* 79, no. 6 (2021): 614-621. <https://doi.org/10.33963/KP.a2021.0003>
- [24] Zieman, Susan J., Vojtech Melenovsky, and David A. Kass. "Mechanisms, pathophysiology, and therapy of arterial stiffness." *Arteriosclerosis, thrombosis, and vascular biology* 25, no. 5 (2005): 932-943. <https://doi.org/10.1161/01.ATV.0000160548.78317.29>